Spin distribution in plastically deformed Fe - Al intermetallic compounds II

Spin distribution in plastically deformed Fe–Al intermetallic compounds II

S Takahashi†, H Onodera‡, X G Li† and S Miura‡

† Faculty of Engineering, Iwate University, Morioka 020, Japan
‡ Institute for Materials Research, Tohoku University, Sendai 980-77, Japan

Abstract. The spin distribution in plastically deformed Fe–Al intermetallic compounds with the compositions of 30 and 35 at.% Al has been studied by Mössbauer spectroscopy and magnetization measurements with high magnetic field. Ferromagnetic clusters along the antiphase boundary (APB) between superpartial dislocations exist even below the freezing temperature and has a strong uniaxial anisotropy. The anisotropy is so strong that the magnetization does not saturate at 4.2 K even with an applied field of 12 MA m^{-1}. The ferromagnetic APB ribbon enhances the neighbouring Fe moments and changes them to the ferromagnetic state. The magnitude of magnetic moments in the APB ribbon is 2.2 μ_B and that of the neighbouring Fe atoms decreases with the distance from the ferromagnetic APB ribbon. The experimental results support our model as the origin of the spin glass in Fe–Al compounds; the paramagnetic state changes to the spin glass under the competition of two clusters with different directions of easy magnetization below the freezing temperature.

1. Introduction

The influence of plastic deformation on magnetic properties has been recently studied in Fe–Al intermetallic compounds with the compositions between 30 and 40 at.% Al (Takahashi *et al* 1996). In the previous study, a new phenomenon in the magnetic anisotropy was found and two models have been proposed by the present authors; one model is concerned with the condition for ferromagnetism and the other is the origin of the spin glass in Fe–Al compounds. This paper is a sequel of the previous study mainly to corroborate the models experimentally by use of the Mössbauer measurements.

   Fe–Al compounds with more than 35 at.% Al concentration are paramagnetic before plastic deformation.   After plastic deformation the magnetic susceptibility increases remarkably and at the same time the spontaneous magnetization, M_s, appears. Plastic deformation induces superlattice dislocations, which contain the antiphase boundary (APB) between them. The atomic configuration in the APB ribbon is different from that of the atomically ordered state. This atom configuration produces the ferromagnetic state. Ferromagnetic clusters are present along the APB ribbons between superpartial dislocations. The change of M_s by plastic deformation, is a simple function of dislocation density, ρ (Takahashi 1986). The relation between M_s and ρ has been examined experimentally, but the experimental value of M_s is 50 times as large as the calculated one in 30 at.% Al concentration. The reasonable explanation for the M_s value is the magnetic influence on the neighbouring Fe atoms. The magnetic influence extends more than 50 atomic distances from the APB (Takahashi *et al* 1996). In the previous estimation, all neighbouring Fe atoms were

considered to carry the magnetic moment of 2.2 μ_B. Actually the spin distribution would depend on the distance from the ferromagnetic APB ribbon. It is of interest to investigate the spin distribution near the ferromagnetic APB ribbon. Mössbauer measurement is one of the best methods to study the spin distribution near the ferromagnetic APB ribbon.

It was found in the previous paper (Takahashi *et al* 1996) that the ferromagnetic APB ribbon has a strong uniaxial anisotropy in 30 and 31 at.% Al concentrations, whose direction of easy magnetization is ⟨100⟩ within the {110} glide plane. The induced magnetic anisotropy has been explained by the same model as the roll-induced magnetic anisotropy in Fe₃Al alloy (Takahashi 1972, 1975). The direction of easy magnetization is intimately related with the atomic configuration of the APB ribbon. The induced magnetic anisotropy is so strong that the magnetization curve in the direction of hard magnetization meets that of easy magnetization in the applied field of 2 MA m^{-1} at 200 K. The induced anisotropy depends on Al content and temperature. The purpose of the present study is to obtain detailed information on the magnetic anisotropy of the APB ribbon, especially at low temperature in a high magnetic field.

The magnetism of Fe–Al compounds is complicated, especially in dependence on Al concentration. The magnetic transition from paramagnetic to ferromagnetic was found at 35 at.% Al concentration. We have introduced one model extending the model of induced magnetic anisotropy to the magnetism of the Fe–Al compound (Takahashi *et al* 1996). The smallest ferromagnetic unit as shown in figure 1 has been proposed to explain the magnetic transition due to the Al content. The direction of easy magnetization in the smallest unit is also the [100] direction connecting the centre site (β-site) Fe–Fe atom pairs as shown in figure 1. The ferromagnetic cluster composed of the smallest unit coexists with the paramagnetic state near the critical concentration of 35 at.% Al. Our interest is the spin distribution of the smallest ferromagnetic unit in the undeformed Fe–Al compounds as well as the deformed ones.
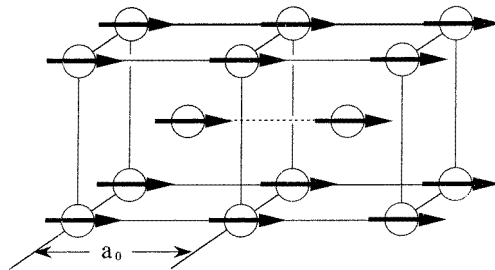

Figure 1. The smallest ferromagnetic unit with a strong uniaxial anisotropy. a_0 is the lattice constant. The direction of easy magnetization is indicated by the arrows.

Fe–Al intermetallic compounds have the spin-glass state at low temperature between 27 and 50 at.% Al concentration. The spin-glass state has been generally explained by the competition between ferromagnetic and antiferromagnetic interactions, so-called 'frustration'. A microscopic model was introduced by Shukla and Wortis (1980). There are two atomic configurations in the B2 type Fe–Al intermetallic compounds as shown in figure 2(a) and (b): Fe atoms occupy the corner site (α-site) and the β-site, and Fe atoms occupy the α-site and Al atoms occupy the β-site. We call these two atomic configurations A- and B-type configurations, respectively, in this paper. There are ferromagnetic and indirect antiferromagnetic interactions between the Fe moments in the A- and B-type
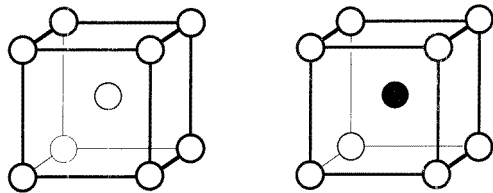
Figure 2. Two kinds of spin distribution in B2-type structure. (a) Fe atoms (○) occupy the α- and β-sites (which is called the 'A-type configuration'). (b) Fe (○) and Al (●) atoms occupy the α- and β-sites, respectively (which is called the 'B-type configuration').

configurations, respectively, according to Shukla and Wortis (1980). In the stoichiometric composition of 50 at.% Al, the atomic structure is composed of the B-type configuration completely, but evidence of the antiferromagnetic interaction could not be obtained, since the Fe moment is very small (Parthasarathi and Beck 1976). One model has been proposed as the origin of the spin glass in the previous study (Takahashi *et al* 1996); the competition of the ferromagnetic clusters with different directions of easy magnetization could be the origin of the spin glass in these compounds. It is also the purpose of the present study to investigate experimental evidence of our model as the origin of the spin glass. The magnetic anisotropy of the smallest unit in figure 1 plays an important role in the model. The anisotropy of the smallest unit is measured in a high magnetic field and the spin distribution near the ferromagnetic clusters is observed by use of the Mössbauer measurement in the present study.

2. Experimental procedure

The raw materials used for alloying were 99.998 mass% Al and 99.95 mass% Fe. Alloy 'buttons' with the nominal composition of 30.0 and 35.0 at.% Al–Fe were prepared by arc melting the raw materials four times to attain chemical homogeneity on a water-cooled copper hearth in an argon gas atmosphere at a pressure of approximately 93 kPa. As weight losses after the arc melting were smaller than 0.1% for an ingot, the nominal composition was regarded as the chemical composition. The buttons were homogenized at 973 K for 2 d. The bulk alloys were rolled at room temperature first until the cracks were introduced. The cold rolling was adopted to make a few slip systems work inhomogeneously. After the cold rolling, the alloys were mechanically reduced to powder of an average size of 40 μm by grinding at room temperature in an agate mortar. The powders with heavy plastic deformation were used for the Mössbauer measurement. Some of the powders were annealed at 1273 K to remove the lattice defects introduced in the grinding process and annealed at 973 K for 2 d for homogenizing. Four kinds of powdered sample were prepared.

The ^{57}Fe Mössbauer spectra on the randomly oriented powder samples were obtained in the temperature range between 4.2 K and room temperature. The Mössbauer effect was measured by an ordinary transmission-type spectrometer with a constant-acceleration driving mode using an Rh(^{57}Co) source. The velocity scale was calibrated using the spectrum of α-Fe metal at room temperature. The spectra with hyperfine field distribution (HFFD) were analysed by the modified Hesse–Rübartsch method (Hesse and Rübartsch 1974) in order to obtain model-independent distribution probabilities.

The magnetization was measured as function of magnetic field using a magnetometer with the vibrating-sample method. The high magnetic fields were produced using a water-
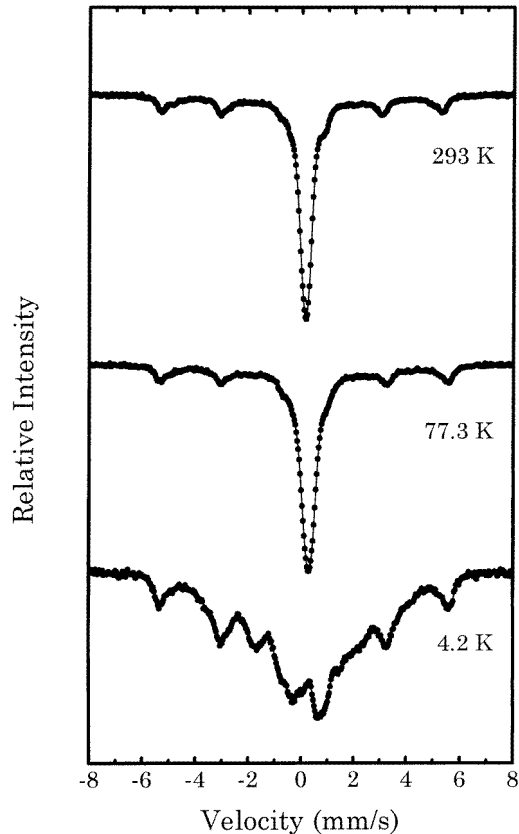
Figure 3. The Mössbauer spectra of 35 at.% Al–Fe compound at 293, 77.3 and 4.2 K. The lattice defects in the sample are removed by annealing.

cooled Bitter-type magnet at the High Field Laboratory for Superconducting Materials (HFLSM) in Tohoku University. The powder sample was sealed in a polytetrafluoroethylene (Teflon) capsule with helium gas and BN powder, and then the sample powder particles were at a homogeneous temperature and were free to rotate in the magnetic field.

3. Experimental results

3.1. Mössbauer effects

Typical spectra for the annealed samples of 35 and 30 at.% Al– Fe compounds are shown in figures 3 and 4, respectively. The critical concentration of paramagnetic and ferromagnetic states is 35 at.% Al. The ferromagnetic state coexists a little in the paramagnetic state at 77.3 and 293 K. The freezing temperature, $T_f = 40$ K in the 35 at.% Al–Fe compound. All the localized moments are frozen at 4.2 K. On the other hand $T_f = 90$ K in the 30 at.% Al–Fe compound, and the ferromagnetic state coexists with the paramagnetic state at 293 K and the localized moments are frozen at 4.2 and 77.3 K.

Figures 5 and 6 show the spectra of the heavily deformed samples of 35 and 30 at.% Al–Fe compounds, respectively. Almost all the magnetic moments of Fe atoms couple
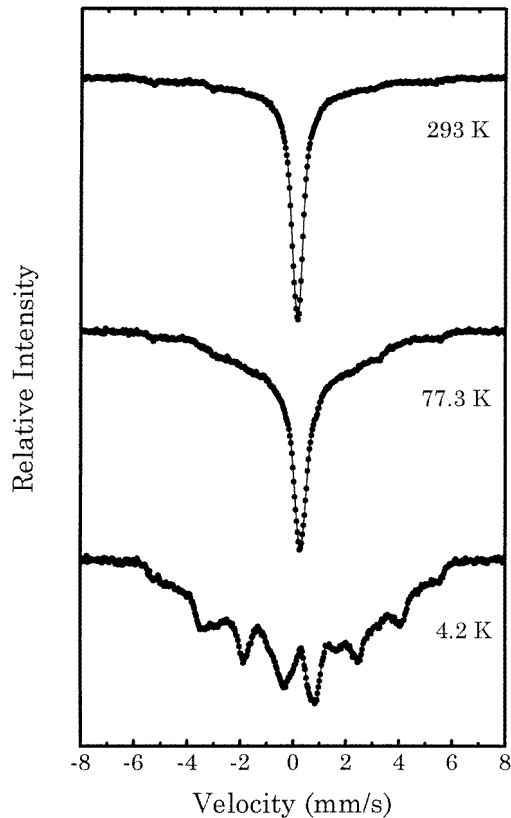
Figure 4. The Mössbauer spectra of 30 at.% Al–Fe compound at 293, 77.3 and 4.2 K. The lattice defects in the sample are removed by annealing.

ferromagnetically; antiferromagnetic coupling is possible, but this possibility will be rejected in the discussion. These spectra were analysed to yield the HFFD probabilities. The magnitude of the hyperfine field corresponds to the magnetic moment per Fe atom; $1 \mu_B = 11.5$–12.0 MA m^{-1}. Figure 7 shows the HFFD of the 35 at.% Al–Fe compound at 293, 77.3 and 4.2 K. The distribution around 26.3 to 27.1 MA m^{-1} is observed at every temperature, which would be caused by the precipitates of Fe atoms. The precipitation would be induced during the annealing. Most of Fe atoms are paramagnetic at 77.3 and 293 K. The ratio of paramagnetic Fe atoms to the total Fe atoms is from 30 to 40%. All the moments are frozen at 4.2 K. Figure 8 is the HFFD of the 30 at.% Al–Fe compound at 293, 77.3 and 4.2 K. The precipitate of Fe atoms is very small compared with the 35 at.% Al–Fe compound. Nearly 30% of Fe moments are paramagnetic and the other Fe moments are magnetically ordered and the moment distributed very widely at 293 K. Paramagnetic Fe moments are also observed at 77.3 K, though $T_f = 90$ K in the 30 at.% Al concentration. The ratio of paramagnetic Fe moments decreases and the frozen moments increase with decreasing temperature. All the moments of Fe atoms are frozen at 4.2 K. The hyperfine field shifts totally to the higher value as the temperature decreases.

Figure 9 is the HFFD of heavily deformed samples of the 35 at.% Al–Fe compound at 293, 77.3 and 4.2 K. The precipitate of Fe atoms is also existent as for the annealed
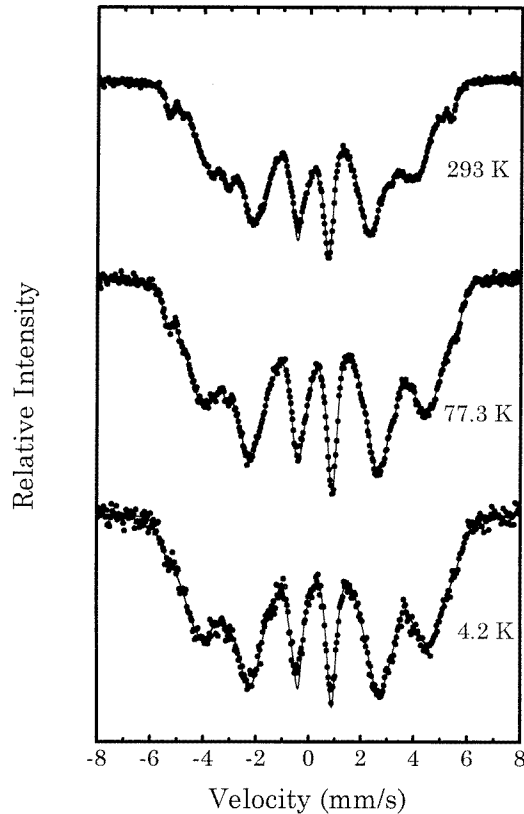
Figure 5. The Mössbauer spectra of 35 at.% Al–Fe compound at 293, 77.3 and 4.2 K. The sample is as crushed.

sample around 26.3 to 27.1 MA m^{-1}. The three HFFDs are similar and do not change clearly in the temperature range between 4.2 and 293 K. Almost all the Fe atoms couple ferromagnetically. Two broad peaks exist at 8.0 and 20.7 MA m^{-1}. Similar HFFDs are obtained in the 30 at.% Al–Fe compound deformed plastically as shown in figure 10.

Figure 11 is the temperature dependence of the averaged hyperfine field. The averaged hyperfine field of the annealed samples decreases rapidly in the temperature range between 4.2 and 75 K in the 35 at.% Al–Fe compound, and between 4.2 and 100 K in the 30 at.% Al–Fe compound. These results correspond well to the spin-glass transitions at 40 and 90 K, respectively. The wide temperature range of T_f is discussed in section 4.1. The averaged hyperfine field in the annealed samples is reversed above 50 K. The reversing phenomenon is caused by the precipitated Fe atoms. The averaged magnetic moments per Fe atom at 4.2 K in the annealed 30 and 35 at.% Al–Fe compounds are 1.2 and 1.1 μ_B, respectively. The averaged hyperfine field increases by plastic deformation in both compounds. The values at 4.2 K of the 30 and 35 at.% Al–Fe compounds are 19.9 and 19.1 MA m^{-1} which correspond to 1.66 and 1.55 μ_B, respectively. They decrease gradually with increasing temperature.
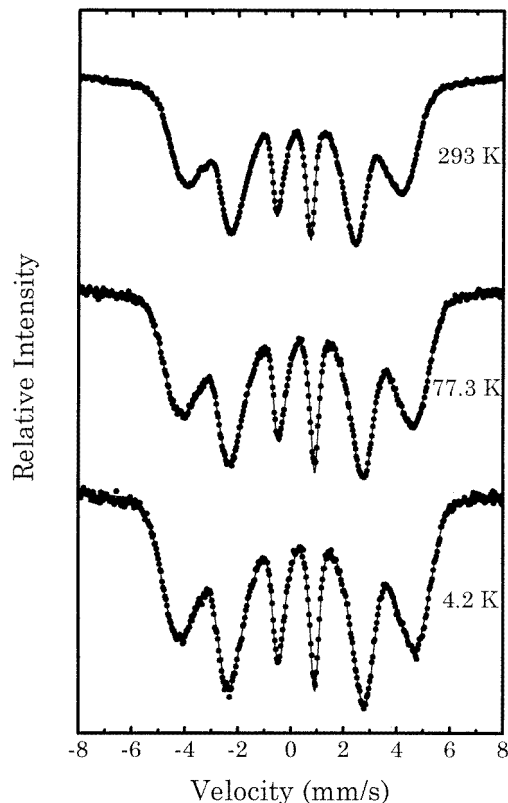
Figure 6. The Mössbauer spectra of 30 at.% Al–Fe compound at 293, 77.3 and 4.2 K. The sample is as crushed.

3.2. Magnetization measurements

Figure 12 shows the magnetization curves at 4.2 K in the annealed sample and the plastically deformed one with 35 at.% Al concentration. The magnetization of the annealed sample is unsaturated even at the applied field of 12 MA m^{-1}. The magnetization curve indicates the coexistence of spin-glass and ferromagnetic states. The localized Fe moments are frozen in the spin-glass state. The unsaturation of magnetization indicates that a strong anisotropy exists in the ferromagnetic state coexisting with the spin-glass state. The averaged magnetic moment per Fe atom obtained from the magnetization at 12 MA m^{-1} is 0.75 μ_B, which is much smaller than that obtained from the averaged hyperfine field. The magnetization of the plastically deformed sample is much larger than that of the annealed one. The magnetization saturates at 0.9 MA m^{-1} and the value of M_s corresponds to 1.5 μ_B in the averaged magnetic moment per Fe atom, which is nearly the same value as obtained by the Mössbauer effect.

Figure 13 shows the magnetization curves at 4.2 K in the annealed sample and the plastically deformed one with 30 at.% Al concentration. The magnetization curves are similar to that for 35 at.% Al concentration. The magnetization of the annealed sample is larger than that for 35 at.% Al concentration. This result is expected, since the ferromagnetic clusters increase with decreasing Al concentration. The magnetization curve
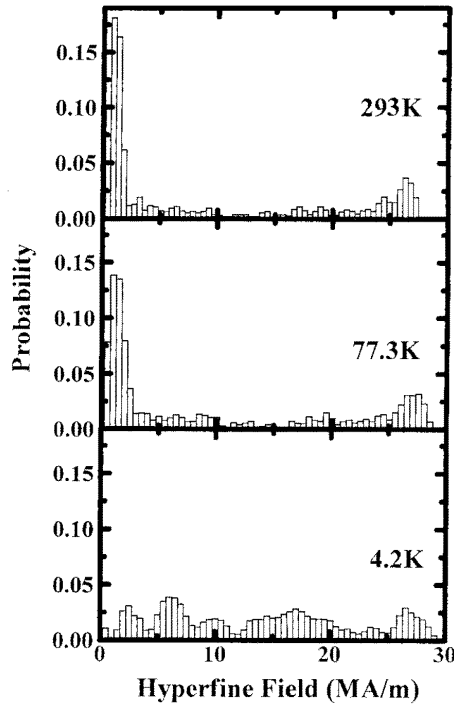
Figure 7. The hyperfine field distribution probability of the 35 at.% Al–Fe compound at 293, 77.3 and 4.2 K. The lattice defects in the sample are removed by annealing.

of the plastically deformed 30 at.% Al–Fe sample seems to saturate at 0.9 MA m^{-1}, but the magnetization is smaller than that for 35 at.% Al–Fe. This result is unexpected. The value of M_s corresponds to 1.25 μ_B in the magnetic moment per Fe atom, which is much smaller than that of the averaged hyperfine field. This phenomenon that the magnetic moment obtained by the magnetization curve is smaller than that of the averaged hyperfine field has been observed previously and becomes evidence of antiferromagnetism in the transition to the spin-glass state (Shiga and Nakamura 1978, 1979).

The averaged magnetic moment per Fe atom has a different value depending on the measuring method. Its value at 4.2 K is shown in table 1.

Table 1. The averaged magnetic moment (μ_B) per iron atom at 4.2 K obtained by two measuring methods, the Mössbauer effect and magnetization curves.

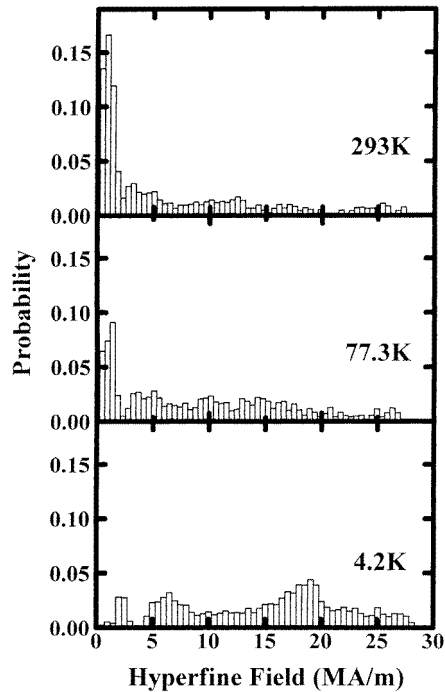| Samples		Mössbauer effect	Magnetization curves
30 at.% Al–Fe compound			
	annealed	1.20	0.84
	as crushed	1.66	1.25
35 at.% Al–Fe compound			
	annealed	1.10	0.75
	as crushed	1.55	1.50

Figure 8. The hyperfine field distribution probability of the 30 at.% Al–Fe compound at 293, 77.3 and 4.2 K. The lattice defects in the sample are removed by annealing.

4. Discussion

4.1. Spin distribution of annealed samples

The annealed samples are regarded as the complete single crystal without lattice defects. The rearrangement of the atoms near the APB begins at temperatures of 373 to 473 K (Huffman and Fisher 1967, Takahashi *et al* 1973). The dislocations are removed by the annealing at 1273 K. The atomic arrangement in the annealed samples is the fully ordered state, though the precipitation of Fe atoms is observed in 35 at.% Al–Fe compound. Each particle of powders is a single crystal, since the mean grain size is 1.1 to 1.3 mm in the button ingot, and the particle size is about 40 μm.

We have introduced one model to explain the spin glass in Fe–Al compounds, i.e. the competition of two ferromagnetic clusters with different directions of easy magnetization (Takahashi *et al* 1996). We explain the present experimental results by our model.

The HFFD indicates that the ferromagnetic clusters coexist with the paramagnetic state at 77.3 K and room temperature in 35 at.% Al. It is also obtained from the HFFD that the ferromagnetic moments distribute over a wide range. The ferromagnetic cluster consists of the smallest ferromagnetic unit as shown in figure 1, and the paramagnetic state consists of the B-type configurations. The other ferromagnetic atom configurations should be introduced to explain the broad HFFD. Fe moments in the A- and B-type configurations would be enhanced to the ferromagnetic state near the smallest ferromagnetic unit. Fe moments near the smallest unit couple ferromagnetically and their magnitude would be smaller than that of the cluster. The magnitude of Fe moments would depend on the size of the ferromagnetic
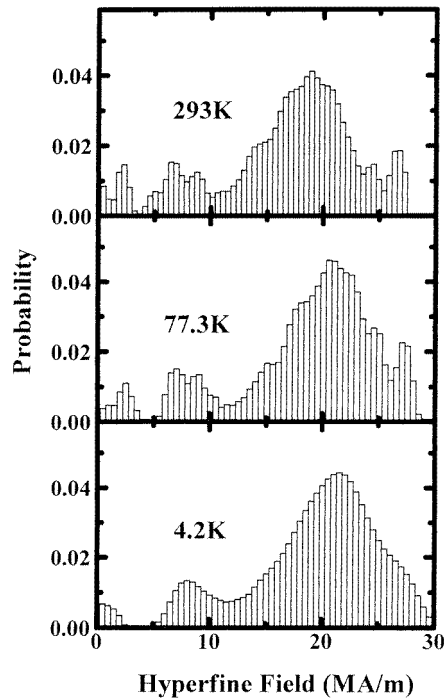
Figure 9. The hyperfine field distribution probability of the 35 at.% Al–Fe compound at 293, 77.3 and 4.2 K. The sample is as crushed.

cluster, the type of configuration and the distance from the smallest unit. The broad HFFD can be explained by the various ferromagnetic atom configurations.

In the spin-glass state, all the Fe moments are frozen and distribute also broadly. We have two possible ideas of the spin-glass state. One is that only the paramagnetic Fe moment changes to the spin-glass state and the ferromagnetic clusters do not change to the spin-glass state but remain. When Fe moments transform from the paramagnetic to the spin-glass state, the moments try to respond to the constraint under the influence of the two neighbouring ferromagnetic clusters with different directions of easy magnetization. The other idea is that all the Fe moments transform to the spin-glass state. If all the Fe moments are frozen at random, the magnetization curve would show different features from the present result, especially in small applied field. The magnetization curves support the former image; the curves have mixed features of the ferromagnetic and spin-glass states rather than the spin-glass one. The unsaturated magnetization indicates the strong anisotropy of the ferromagnetic clusters as well as the spin-glass state. The critical concentration where the spin-glass state appears is 27 at.% Al, which would be the critical concentration where the paramagnetic state appears in the ferromagnetic state.

Above the critical concentration of 27 at.% Al, the ferromagnetic clusters are directly connected with each other. Each cluster has its own direction of easy magnetization, i.e. one of the ⟨100⟩ directions. A large cluster is composed of small clusters with different directions of easy magnetization. The individual ⟨100⟩ directions of easy magnetization are unified to the three ⟨100⟩ directions; every Fe moment has three ⟨100⟩ directions of easy magnetization in the large cluster. This is the origin of the magneto-crystalline anisotropy in
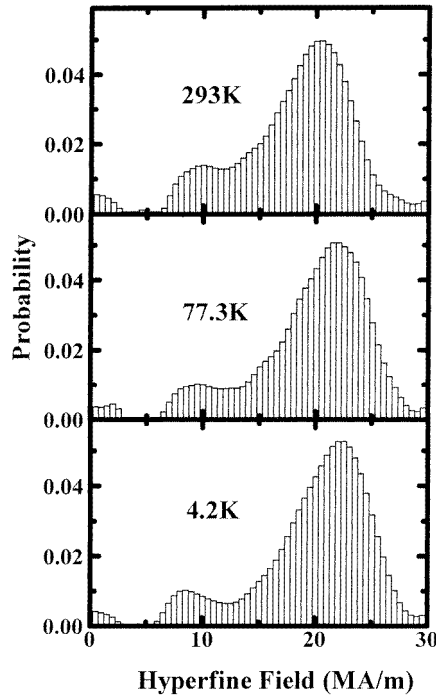
Figure 10. The hyperfine field distribution probability of the 30 at.% Al–Fe compound at 293, 77.3 and 4.2 K. The sample is as crushed.

the B2 type Fe–Al compounds. Fe_3Al alloy has the DO_3-type structure as well as B2 type. There exists no smallest ferromagnetic unit in the DO_3-type structure. The direction of easy magnetization is $\langle 111 \rangle$ in the magneto-crystalline anisotropy of the DO_3-type structure; the A-type configurations line up in the $\langle 111 \rangle$ directions, whose symmetry produces the $\langle 111 \rangle$ direction of easy magnetization. We can make the smallest units in the DO_3-type structure artificially by the magnetic annealing effect and observe the induced anisotropy with a $\langle 100 \rangle$ direction of easy magnetization (Taniguchi and Yamamoto 1954).

The strong uniaxial magnetic anisotropy can be a clue to explain the difference of the averaged Fe magnetic moments between Mössbauer effect and the magnetization measurement. The ferromagnetic clusters with three $\langle 100 \rangle$ directions of easy magnetization exist with the same probability in each particle. One of the $\langle 111 \rangle$ directions of the particle turns to the applied magnetic field in the magnetic measurement, since particles can rotate freely. The magnitude of magnetization in the initial stage of the magnetization curve is $(1/\sqrt{3})$ times the magnetic moment obtained from the averaged hyperfine field. The present experimental results show a good agreement with the above idea. The small difference would be caused by the spin-glass state.

The magnetization curves increase clearly with increasing applied field and never saturate even in the applied field of 12 MA m^{-1}. The anisotropy of the ferromagnetic cluster is so strong that the magnetic moments deflect from the direction of the applied field even in the 12 MA m^{-1} field.

The HFFD indicates that the paramagnetic state occupies more than 30% of the total Fe moments just above T_f at 35 at.% Al concentration. At 30 at.% Al concentration, the
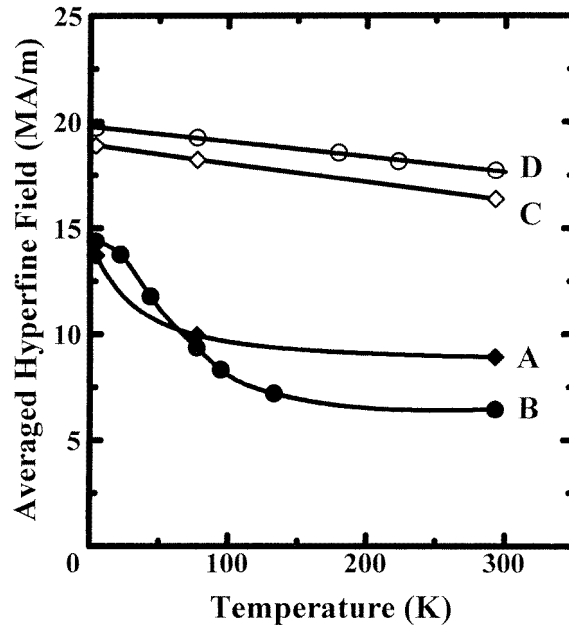
Figure 11. The temperature dependence of the averaged hyperfine field. A: the annealed 35 at.% Al–Fe sample, B: the annealed 30 at.% Al–Fe sample, C: as the as-crushed 35 at.% Al–Fe sample and D: the as-crushed 30 at.% Al–Fe sample.

paramagnetic state is observed even at 77.3 K and it is transformed to the spin glass at 4.2 K. Fe moments in the B-type configuration should be paramagnetic, which are transformed to the spin glass below T_f.

In the 30 at.% Al–Fe compound, the paramagnetic state appears at 77.3 K below T_f (=90 K) as well as at 293 K. Fe moments in the paramagnetic state are frozen completely at 4.2 K. The observed spin glass is composed of states with the different values of T_f. The spin-glass state has its own value of T_f. The value of T_f depends on the distance from the neighbouring ferromagnetic clusters: T_f becomes high as the distance decreases. The measured value of T_f is the averaged one, which was observed as a broad peak in the magnetic susceptibility versus temperature (Okamoto and Beck 1971, Takahashi *et al* 1996). The wide temperature range of T_f corresponds to the rapid decrease of the averaged hyperfine field in the wide temperature range near T_f, as shown in figure 11.

4.2. Spin distribution of plastically deformed samples

The samples were hardly deformed by cold rolling at first. There are six slip systems, $\langle 111\rangle\{110\}$, in Fe–Al compounds. A few of these slip systems would be contributed to the plastic deformation in each single grain, during the cold rolling. Each particle is a single crystal deformed inhomogeneously.

The value of ρ in the powder sample is difficult to obtain by direct methods such as the electron microscope. It is possible to obtain ρ indirectly by the relation between ρ and the increase of M_s (Takahashi 1986). In this method, the influence of the ferromagnetic APB ribbon on the neighbouring Fe atoms should be considered and n is defined as the influenced
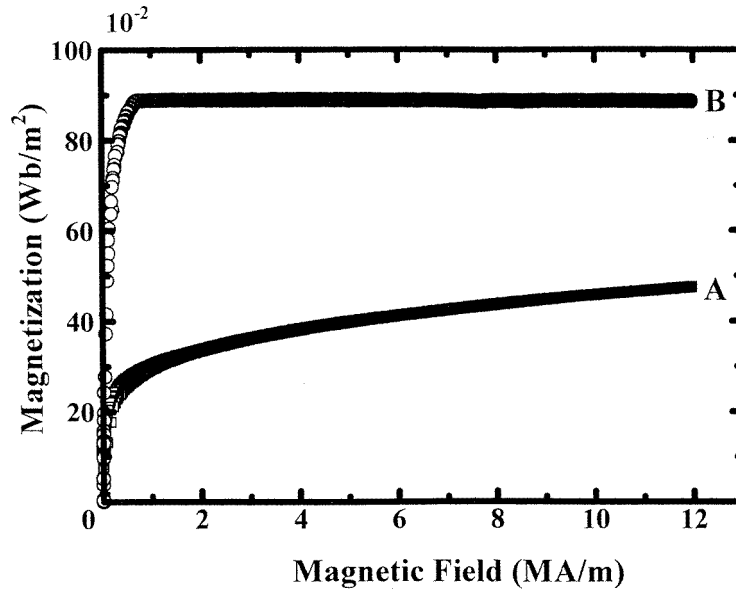
Figure 12. The magnetization curves of the 35 at. % Al–Fe compound at 4.2 K, A: the annealed sample, B: the as-crushed sample.
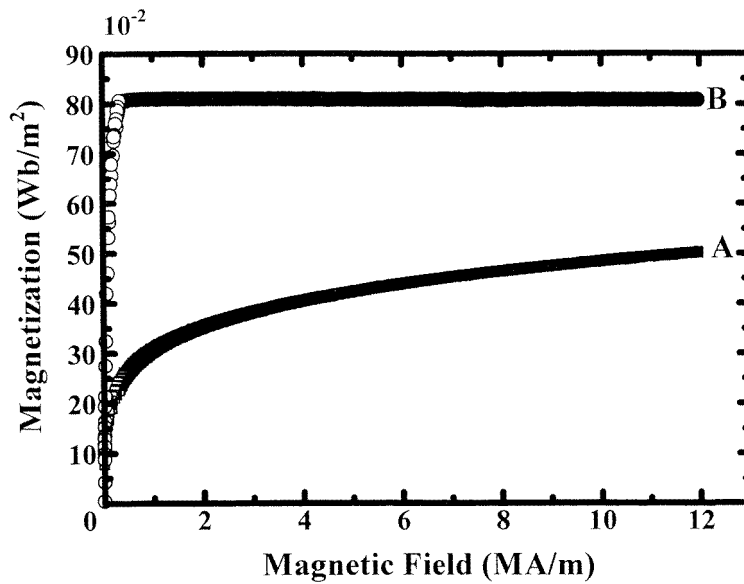

Figure 13. The magnetization curves of the 30 at.% Al–Fe compound at 4.2 K, A: the annealed sample, B: the as-crushed sample.

distance; the magnetic transition from paramagnetism to ferromagnetism is extended as far as the nth-NN distance from APB. The magnetic influence extends to $n = 50$ in the 30 at.%

Al–Fe compound, when all the Fe atoms within 50th-NN from the APB carry the magnetic moment of 2.2 μ_B. We can obtain the dislocation density $\rho = 10^{11-12}$ cm^{-2}. In fact, the magnetic moment of the neighbouring Fe atoms would be smaller than 2.2 μ_B. The magnetic moment of Fe atoms near the APB ribbon would be reflected in the broad HFFD.

The HFFD changes considerably between the two samples, the as-crushed one and the annealed one. The introduction of ferromagnetic APB ribbons in the spin-glass state changes the spin distribution considerably. We cannot observe a clear change in the HFFD at 4.2 and 293 K in two Fe–Al compounds. The similar spectra lead us to the conclusion that the spin-glass state does not remain in the as-crushed sample at 4.2 K. Even if it remains, the ratio would be very small. When the sample is not deformed so hard, the spin-glass state remains below T_f (Takahashi *et al* 1996).

The averaged distance between the APB ribbons, r_{APB}, is estimated from the value of ρ, i.e. $r_{APB} = \sqrt{2/\rho}$ and $r_{APB} = 10$ to 20 nm can be obtained. The magnetic influence of the APB ribbon on the neighbouring Fe moments can be obtained on the supposition of Gaussian distribution. The ferromagnetic state extends to about 15 nm around the APB ribbon. This estimation supports the above consideration that there exists only the ferromagnetic state in the crushed samples. Four ferromagnetic structures would be considered in the as-crushed samples, the ferromagnetic APB ribbon and two kinds of ferromagnetic cluster consisting of A-type and B-type configurations and the ferromagnetic smallest unit. The broad spectrum indicates that the four magnetic structures interact with each other and that the ferromagnetic APB ribbons decide the fundamental magnetic structure in the as-crushed samples, since the introduction of ferromagnetic APB ribbons changes the spectrum considerably. The ferromagnetic APB ribbon exerts influence on the neighbouring Fe moments. Fe atoms would carry the magnetic moment of 2.2 μ_B just near the APB ribbon. Fe moment would decrease with the distance from the APB ribbons, depending on the A- or B-type configuration. The HFFD around 8.0 MA m^{-1} would be caused by the Fe moments of the B-type configuration which are located farthest from the neighbouring APB ribbons.

The averaged magnetic moment obtained by the magnetization curve is smaller than that of the averaged hyperfine field, especially in 30 at.% Al concentration. The unexpected result is found in the magnetization curves of the as-crushed samples; the magnetization at 30 at.% Al concentration is smaller than that of 35 at.% Al, though the averaged hyperfine field at 30 at.% Al concentration is larger than that of 35 at.% Al. We explain these two experimental results. When $[\bar{1}11](110)$, $[1\bar{1}1](110)$, $[\bar{1}11](101)$ and $[11\bar{1}](101)$ slip systems work, for example, in the cold rolling, the APB between superpartials is induced over the (110) and (101) glide planes. The directions of easy magnetization in the ferromagnetic APB ribbon are [001] in the $[\bar{1}11](110)$ and $[11\bar{1}](110)$ slip systems and [010] in the $[\bar{1}11](101)$ and $[11\bar{1}](101)$ slip systems. Each particle contains ferromagnetic APB ribbon with strong uniaxial magnetic anisotropy, whose directions of easy magnetization are two of the three $\langle 100 \rangle$ directions.

Each particle would rotate to such a direction in the magnetic measurement that the $\langle 110 \rangle$ between the two $\langle 100 \rangle$ directions of easy magnetization turns to that of the applied magnetic field. The induced anisotropy of the 30 at.% Al–Fe compound is so strong that the magnetic moment does not turn to the $\langle 110 \rangle$ direction even in an applied field of 12 MA m^{-1}. The averaged magnetic moment is observed as reduced in the magnetization measurement by $1/\sqrt{2}$, compared with the moment due to the averaged hyperfine field. The magnetic anisotropy of the smallest unit would be influenced by the neighbouring APB ribbon and has the same direction of easy magnetization as that of the APB ribbon. The magnetic anisotropy of the smallest units is also so strong that they do not turn to the direction of the applied field in the 30 at.%Al–Fe compound. The magnetic anisotropy decreases with

increasing Al concentration. In the 35 at.% Al–Fe compound, the magnetic moment turns to the ⟨110⟩ direction easily in the applied field. The large difference of the magnetic moments by the two methods is not observed in the 35 at.% Al–Fe compound. We can explain the unexpected result by the above consideration.

The difference of magnetic moments by the two measuring methods is observed in the 35 at.% Al, though it is smaller than that of 30 at.% Al–Fe. The magnetic anisotropy of the neighbouring Fe moments at 35 at.% Al concentration is not so strong as at 30 at.% Al. The moments of the neighbouring Fe moments turn easily to the direction of applied field but those of the APB ribbons do not turn in the 35 at.% Al–Fe compound. The strength of the magnetic influence decreases with increasing Al concentration.

The averaged magnetic moment obtained by the magnetization measurement in the previous investigation is larger than that of the present study, though the particle size is nearly the same; the averaged magnetic moment is 2.0 μ_B at 29.9 at.% Al concentration (Besnus *et al* 1975). Since the powdering methods are different, the dislocation density and its distribution are different in these samples. Detailed study on the dislocation structure would be necessary to explain the difference of the averaged moments in these studies.

Acknowledgments

References

Besnus M, Herr A and Meyer A J 1975 *J. Phys. F: Met. Phys.* **5** 2138
Hesse J and Rübartsch A 1974 *J. Phys. F: Met. Phys.* **7** 526
Huffman G P and Fisher R M 1967 *J. Appl. Phys.* **38** 735
Okamoto H and Beck P A 1971 *Metall. Trans.* **2** 569
Parthasarathi A and Beck P A 1976 *Solid State Commun.* **18** 211
Shiga M and Nakamura Y 1978 *J. Phys. F: Met. Phys.* **8** 177
——1979 *J. Physique* **3** 204
Shukla P and Wortis M 1980 *Phys. Rev.* B **21** 159
Takahashi S 1972 *Phys. Status Solidi* **52** 141
——1975 *Phys. Status Solidi* **69** 227
——1986 *J. Magn. Magn. Mater.* **54–56** 1065
Takahashi S, Hayashi S and Yamamoto M 1973 *J. Phys. Soc. Japan* **34** 2734
Takahashi S, Li X G and Chiba A 1996 *J. Phys.: Condens. Matter* **8** 11 243
Taniguchi S and Yamamoto M 1954 *Sci. Rep. Res. Inst. Tohoku Univ.* A **6** 336